

SOURCE ANALYSIS OF NEAR-FIELD EARTHQUAKE RECORDS OBSERVED IN ROCK SITES

N HORI¹, S YAMAMOTO² And M YAMADA³

SUMMARY

We obtained the aftershock velocity records on the several rock sites in the epicentral region of the main shock, 1995 Kobe (Hyogo-ken Nanbu) earthquake. The fault-plane solutions for some aftershocks were estimated by using 3-component records of a single observation site. Since many records clearly showed P and S polarities without being contaminated by path-effect, the fault-plane solutions were calculated from the records on the assumption that wave-field was the half-space and target faults were double-couple point sources. Calculated results almost agreed with existing active faults around the epicentral regions and this indicates an important role of a source radiation in near-field seismic motions. The seismic source spectrums were also obtained from the several near field records. These events were shallow earthquakes and the hypocentral distances were from 7 to 11km. The faults-length estimated based on the moving source assumption harmonize with the magnitudes.

INTRODUCTION

The Kobe earthquake was an inland type which had the hypocenter in the vicinity of Akashi strait and the rupture in the fault plane spreaded to Awaji island northern part and directly under Kobe City. According to the Japan Meteorological Agency (JMA) the occurred time was 5:46:52 (JST) on January 17, 1995 and the hypocenter was the north latitude 34.61°, longitude 135.04°, 14.3km depth. [Kikuchi 1995] analyzed the wave inversion by using the displacement records of the broad band seismograms and decided the fault-plane solution and the source process at that day of the main earthquake. According to the report, the dislocation consisted of right strike slip and three sub-events, and the earthquake moment was 2.5×10^{19} Nm (M_w 6.9). The main shock showed the ground surface fault over 10.5km along with the Nojima active fault of Awaji island [Nakata and Yomogida 1995]. The source fault occurred in the shallow place and there were outcrops of the base rocks in the near field. Then we observed the aftershocks on the granite bedrock in the near field from January 18 to February 20, 1995. There were possibilities that the pass effected little to the records on the rock and the radiation property was contained strongly.

The purposes of this paper are as follows

- 1) Analysis of aftershock data observed on rock.
- 2) Determination of the fault-plane solution for the aftershock record in the near field.
- 3) Determination of fault length of the aftershock in the near field based on a moving source model.

AFTERSHOCK OBSERVATION

Observation Points

We observed on the following six points. They are Okuyama, Ashiya City (OKU), East Maruyam, Nagata, Kobe City (MARU), Fukiai, Chyuou-ku, Kobe City A (FUKIA), B (FUKIB), C (FUKIC), and Hirabayashi, Nojima, Hokudan City (HIRA). Geological features are all cropouts of granite or the granodiorite in the Cretaceous or Pre Cretaceous. The details are as follows; (OKU): An average microtremor level was 400 kine or less,

¹ Faculty of Engineering, Kokushikan University, Tokyo, JAPAN, Email: hori@kokushikan.ac.jp

² National Research Institute for Earth Science and Disaster Prevention, Ibaraki, JAPAN, Email: syama@geo.bosai.go.jp

³ Advanced Research Institute for Science and Engineering, Waseda University, Tokyo, JAPAN, Email: yamadamk@mn.waseda.ac.jp

(MARU): Geological features were cropouts of the weathering granodiorite (Before the cretaceous). Since there were many traffics, the microtremor level was as higher as 1000 kine grade, (FUKIA): The microtremor level was about 500 kine grade, there were sometimes a passing car or persons, (FUKIB): The microtremor level was about 200-400 kine, (FUKIC): The point was a fresh granodiorite, and the microtremor level was 400 kine or less, (HIRA): The point was a cropout of the Nojima granodiorite (Cretaceous) and was the quarrying place. During the observation period, there were little artificial source in the vicinity and the microtremor level was 400 kine or less. The positions of each observation points and active faults are shown in Fig.1.

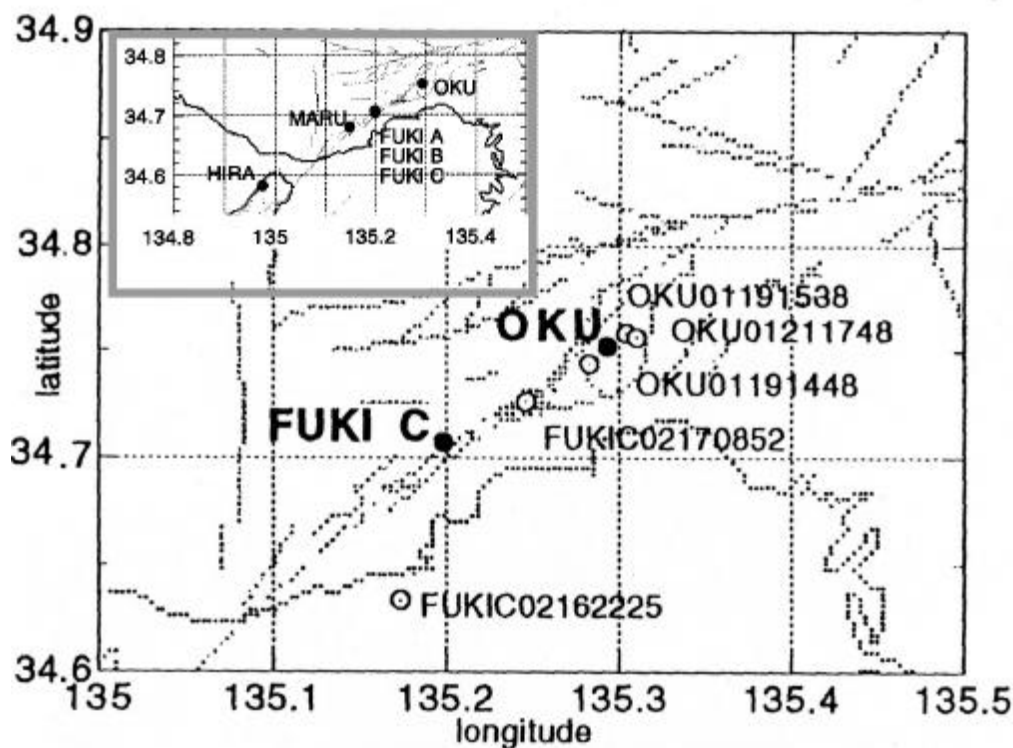


Figure 1: Locations of observation points and aftershocks

Observation System and Microtremors

The observations were performed using a portable seismograph with the servo type velocity sensor of three components. The sensor has the flat characters in 0.5-40Hz. The resolution of A/D is 16bit (80db or more). Sampling rate was 200Hz, full-scale was 100mkine, the trigger condition was 1.0-2.0mkine and delay-time was 2.5sec. The peaks of the Fourier spectrums of microtremors are distinguished in the range 1-2Hz at OKU, MARU, FUKIB, in the range 1.5Hz and 3Hz at FUKIC, and in the range 8-10Hz at HIRA, respectively. It is difficult to distinguish the cause whether these dominant frequencies depend on the amplification of the surface ground or depend on the characteristic frequencies in the microtremor sources. However, these peaks have no effect on the velocity spectrums of the aftershock record. Then these effects are ignored in the following analyses.

Hypocentral Positions of Observed Records

The total numbers of recorded files was about 900 and the continuous observation time exceeded 360 hours. The hypocenter positions of the aftershocks of which magnitudes were large have been decided by some organizations. For example, JMA, Earthquake Research Institute The University of Tokyo (ERI), Institute of the Disaster Prevention, the Kyoto University, and the investigate headquarters of the earth's crust activity to Hyogoken Nanbu earthquake reported. Comparing the triggered time of the recorded aftershocks with the ones reported by [ERI 1995], 363 seismic records were selected from the total records. Those hypocenter positions are plotted in Fig.2. The recorded aftershocks concentrate on the vicinity of FUKIB since the observation period in FUKIB was longer than those in other's points. However, the places coincide with the source of the main shock. The distribution spreads over about 40km and 15km depth and the strike angle is about N50E.

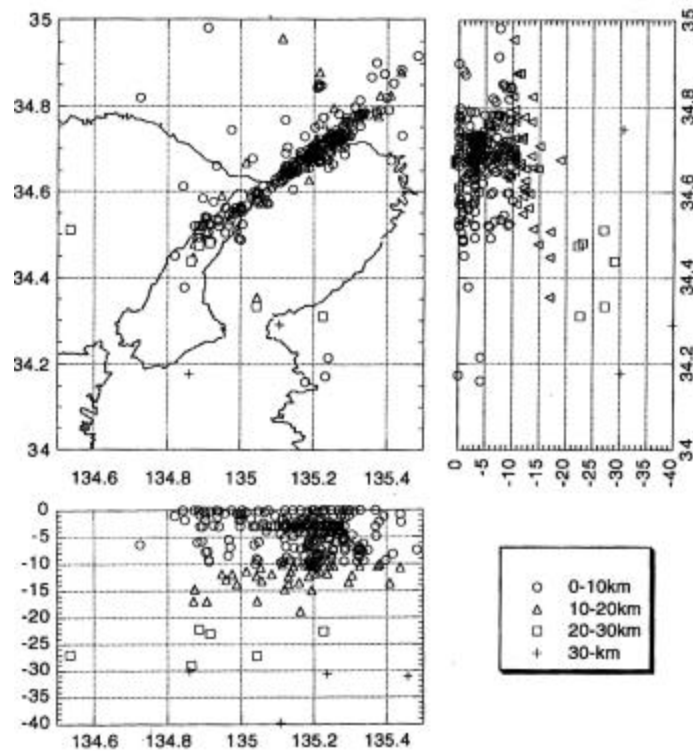


Figure 2: Hypocenters of recorded aftershocks for the period Jan. 18 –Feb. 20 1995 on the rock-sites.

WAVE FORM ANALYSIS OF AFTERSHOCK

The selected aftershocks herein are shown in Table 1. The epicenter distances are 5 km 15 km which are estimated from the time differences of P-S. The maximum magnitude decided by the JMA is 3.8. These satisfied the following conditions.

- 1) The difference at time when the first motions of P-wave and S-wave arriving respectively is 2 sec or less,
- 2) The maximum amplitude is 10mkine or more,
- 3)The maximum amplitude of P-wave is greater than that of S-wave $\bar{0.5}$.

A wave form is shown in Fig.3. The maximum amplitudes, the differences of P-S arriving-time, and the distances of the hypocenters were shown in Table 2. The zero line of the velocity record was corrected and displacement was obtained. The zero line was corrected again. At this time, the running average was removed. The width of the average window was assumed to be 1sec. 3-dimensional particle motion at one cycle was drawn from P-wave initial motion and incident angle and back-azimuth were calculated. The ground structure was assumed as an elastic half space and the velocities of P-wave and S-wave were 5500m/sec and 3200m/sec, respectively. The obtained incident angles are 26° or less measured from a perpendicular axis. The P-S converted waves are distinguished by OKU01191448. Since the hypocentral distance of OKU01191448 is 7.5km and the incident angle is 6°, it is presumed that there is a reflection layer in the ground structure right under the observation point. However, according to the ground velocity values by blasting experiment in the past [Yoshii and et al. 1973], we assumed that the influence of the sound impedance ratio of the layer structure was small.

Table 1: Aftershocks used in this study

Event name	Site	Date	Time	Latitude (°)	Longitude (°)	Depth (km)	Magnitude (*)
OKU01191448	OKU	Jan.19	14:48:16	34.744	135.283	7.3	2.5
OKU01191538	OKU	Jan.19	15:38:44	34.758	135.304	6.7	2.8
OKU01211748	OKU	Jan.21	17:48:32	34.757	135.31	9.2	2.4
FUKIC02162225	FUKI C	Feb.16	22:25:48	34.633	135.174	7.1	3.1
FUKIC02170852	FUKI C	Feb.17	8:52:00	34.726	135.246	7.4	2.6

(*) : After JMA

Table 2: characters of wave forms and faults.

Event name	Max. velocity (kine)	P-S time (sec)	Hypocentral distance (km)	Incident angle (°)	fo(P-wave) ()	fo(S-wave) ()	Fault length by fo(P)(m)	Fault length by fo(S)(m)
OKU01191448	22(hor.*S)	0.98	7.5	6	6	5	127	156
OKU01191538	25(ver.**S)	0.89	6.8	17	6.1	6	176	271
OKU01211748	11(ver.P)	1.27	9.3	22	10	9.2	80	93
FUKIC02162225	25(hor.S)	1.44	11	26	20	12	52	124
FUKIC02170852	33(hor.S)	1.15	8.8	16	23.3	18	49	108

(*) : Horizontal component, (**) : Vertical component

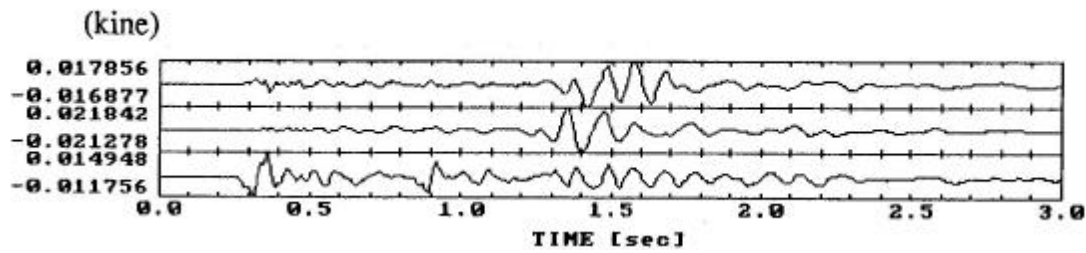


Figure 3: An example time-history (OKU01191448) of observed records

ESTIMATIONS OF FAULT-PLANE SOLUTIONS FOR AFTERSHOCKS

Method of Estimation of Fault-Plane Solution

In this study, the fault-plane solution is estimated by using the seismic waves observed at one point. The fault-plane solution is usually presumed by the pushing and pulling of P-wave's first motion recorded at two or more observation points. However, since the observation point is one point in this paper, the analysis using 3 dimensional vector of the first motions of P-wave and S-wave's one is proposed. The estimated parameters are hypocenter's position, strike angle (), dip angle (), and rake angle (). The analysis is consisted from two steps. The hypocenter position is calculated in the first step. In the second step, the source parameters are obtained. The details are as follows.

(The first step)

The directions of the incident waves are obtained from the polarities and the 3-dimensional vectors of the pushing and pull of the P-waves. Next, the hypocenter position is decided by assuming the ground structure, and considering the difference of the time between the P-S arrivals.

(The second step)

The source parameters are gradually changed and the values, which can best explain the 3-dimensional vectors of the initial P-wave motions and S-wave motions, respectively, are calculated. It is evident that the angle between calculated P-wave vector and observed one is 0° or 180° because of the first step's assumption. Therefore, the converging conditions actually used consist of the polarity of P-wave and the angle between the calculated S-wave vector and the observed one. Because the lengths of the targeted faults are enough small to the hypocenter distances, the approximate solution in the far field was used as a source.

Restraint Conditions and Soil Structure Model

Because the fault mechanisms in Kobe and the Awaji regions were right strike slips with a large dip angle, the fault-plane solution was obtained from the condition that the dip angle is constrain from 60° to 90°. The elastic half space model and the two layer elastic model were prepared as a soil structure model. V_p , V_s , and ρ of the elastic half space model are 5500m/sec, 3200m/sec and 2.5g/cm³, respectively. In the case of 2-layer elastic model, the values of 1st layer are 5000m/sec, 2500m/sec, 2.2g/cm³ and the values of 2nd layer are 5500m/sec, 3200m/sec, and 2.5g/cm³. The thickness of 1st layer of the 2-layer model is 5.0km. Moreover, Q-values were assumed as to be infinite in all layers. The difference between the results using those assumptions in the preliminary analysis was little. Then, the results using the elastic half space model are shown in the following analysis.

Analytical Results

The records to be able to clearly reading the initial motions of P-wave and S-wave were used for the analysis. The calculated results of the hypocenter positions and the fault parameters are shown in Table3. The focal mechanism is corresponding to a fault plane or an auxiliary plane. The estimated hypocenter positions are within the several km errors. The positions decided by the JMA are different to the ones decided by another organizations. Then these errors can be regarded as to be small. The errors between the calculated S-wave vectors and observed values are less than 25° except one case. Fig.4 show the calculated fault-plane solutions (the upper hemisphere) for station OKU. The dashed lines in figure show the active fault positions. The results are based on the assumption that the slip is right strike. The calculated angles coincide to the angles in the active faults and strike angle of the main earthquake. It is also shown that the initial motion of the S-wave maintains the source radiation characters strongly.

Table 3 Fault-plane solutions obtained by body-wave inversions

Event name	Latitude (°)	Longitude (°)	Depth (km)	(°)	(°)	(°)	Error (°)
OKU01191448	34.744[0.019]	135.283[0.014]	7.3[-4.3]	95	80	30	8
OKU01191538	34.758[0.05]	135.304[0.051]	6.7[-1.3]	275	80	340	9
OKU01211748	34.757[-0.003]	135.31[-0.051]	9.2[-1.2]	195	90	200	18
FUKIC02162225	34.633[-0.025]	135.174[0.008]	7.1[-5.4]	150	60	320	53
FUKIC02170852	34.726[-0.004]	135.246[0.076]	7.4[-5.4]	300	60	40	24

[] : Error between this study and JMA value

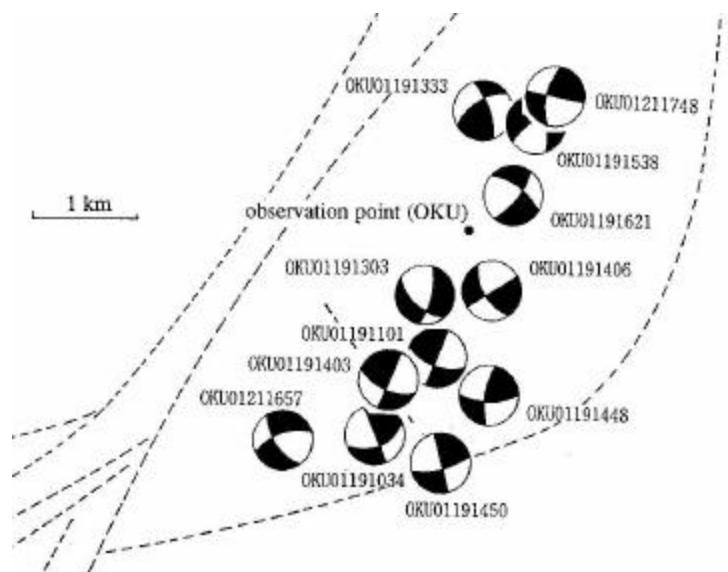


Figure 4 Calculated fault-planes in this study (at OKUYAMA)

5. SOURCES SPECTRUMS AND CORNER FREQUENCIES

5.1 Source Spectrum

Using the incident angle and the direction of the arriving wave motion obtained by the above analysis, the displacement record was separated to longitudinal (P) component: L, vertically polarized (SV) component: Q, and transversely polarized horizontal (SH) component: T. The displacement spectrum densities were obtained from the L component of P-wave and the T component of S-wave (Fig.5). The dispersion's influence through the pass was disregarded since the hypocentral distances of the aftershocks were less than 11km and above chapter 4's analysis. $Q = \dots$ was also assumed. Fig.5 shows the flat characters in the low frequency range less than 10Hz. The data in the range 40Hz or less can be used for the analysis from the seismograph's restriction.

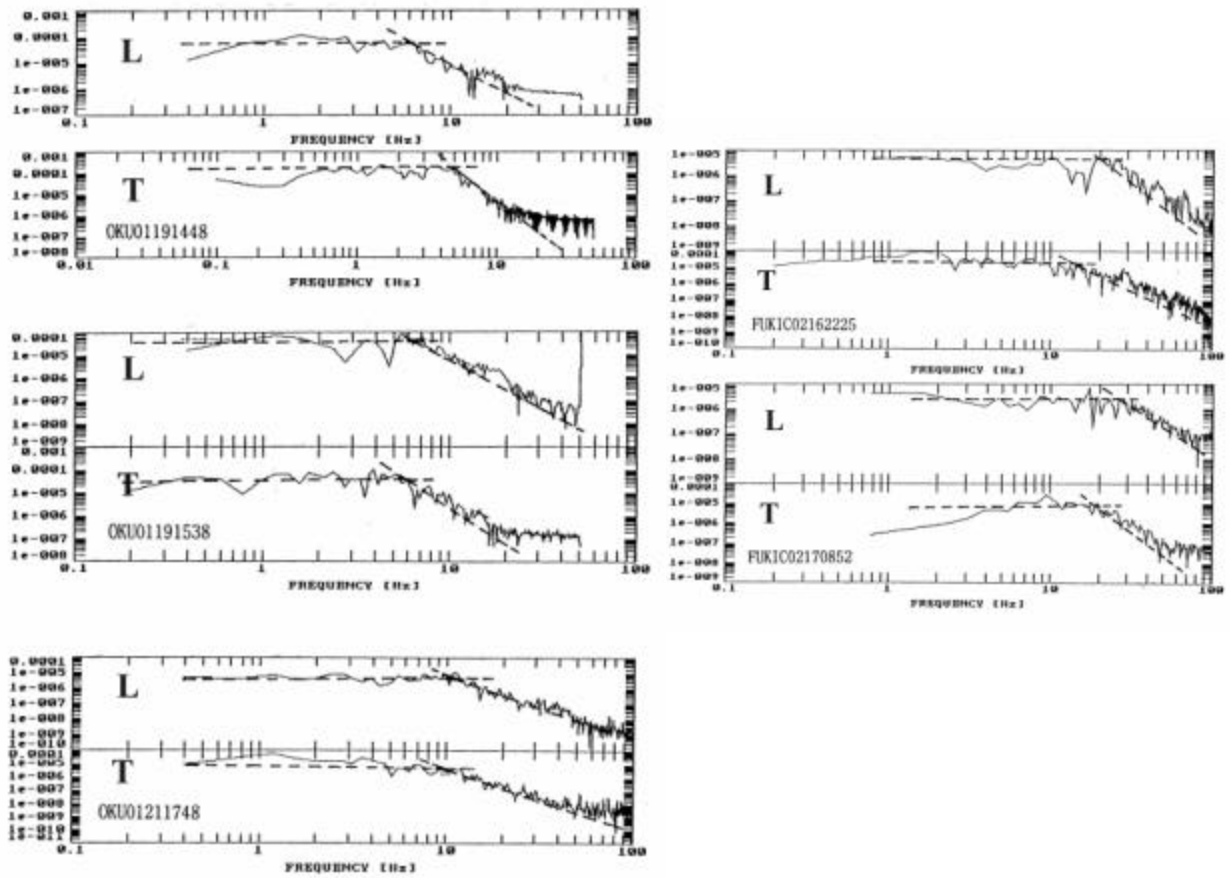


Figure 5: Spectral densities of observed waves

Corner Frequency

The uni-lateral moving source model with finite length was assumed and the fault lengths were calculated from the spectrums. The corner frequencies obtained from Fig.5 are shown in Table 2. The inclinations of the envelop curves in the high frequency range exist in ω^{-1} and ω^{-2} and the following expression presents the directivity from the moving source to the observation point's azimuth.

$$L = 2c / [2\pi f_0 (c / V_r - \cos \theta_1)] \quad (1)$$

where L is the fault length, c is the elastic propagation velocity from the source to the observation point, f_0 is corner frequency, V_r is the rapture velocity of source and θ_1 is the direction angle from the source to the observation point. The rapture velocity is assumed to be $V_r = 0.72c$. θ_1 was calculated by using the source parameters - the strike, dip and rake angles in Table 3. Then angle θ_1 , measured in anti-clockwise direction from the direction of the rapture propagation to the observation point, is provided and the length L is calculated from Eq.1 and the results are also shown in Table 2. The fault lengths were obtained from P-wave and S-wave respectively.

Though the length obtained from S-wave is larger than ones from P-wave, the difference between them is small. The relations between the obtained fault lengths and the magnitudes (JMA) are shown in Fig.6 (a) and (b). The error bar in figures show the variance depending on $0 < \theta_1 < 90^\circ$.

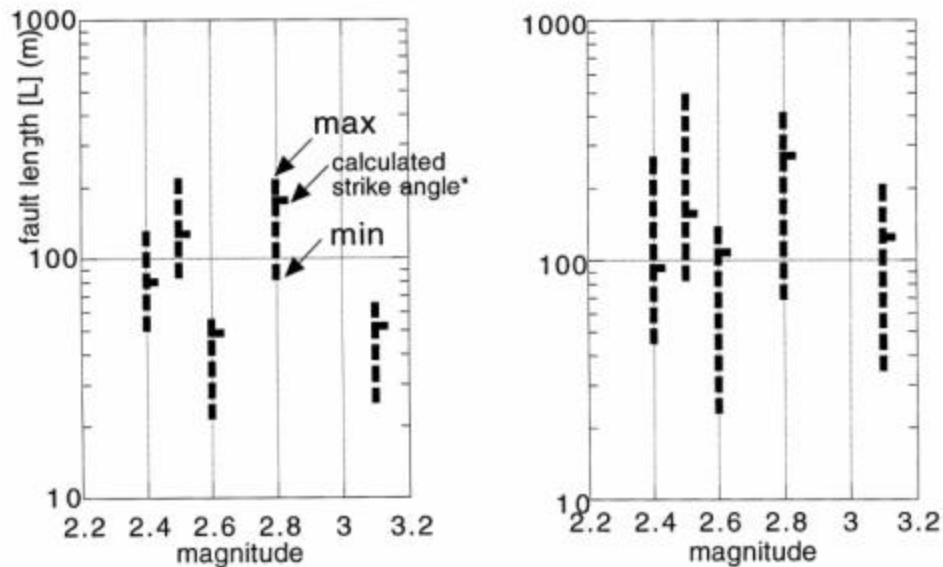


Figure 6: (a), Fault length estimated by P-wave corner frequencies, (b), fault length estimated by S-wave corner frequencies.

CONCLUSIONS

The aftershock observations were done on the rocks in Kobe and Awaji after Kobe earthquake and about 900 aftershocks were recorded. The several hundreds seismic waves which had the epicentral distances within 16km were recorded. Using the obtained records, we analyzed the spectra characters, the fault-plane solutions, the corner frequencies and the fault lengths and the following conclusions were obtained.

- 1) The seismic waves recorded on the bedrock also include the amplificative characters of the rock feature. However, we eliminated several hundreds data and got 6 data which could explain the source characters.
- 2) Using the initial motions of P-wave and S-wave at one point, the fault-plane solutions of the aftershocks were analyzed. These results harmonized with the known active faults and the mechanism of the main shock. It shows that the initial motion of the observed S-wave maintains the source radiation characters.
- 3) The corner frequencies were obtained. The fault lengths based on the moving source model were calculated and agreed with the values predicted from magnitude 2.4-3.1 (JMA) earthquakes.

ACKNOWLEDGEMENTS

The traffic situation and the communication situation etc. were very bad in the hypocentral region immediately after the main shock. The many pre-observations and the continuous observations might not be able to do without the help of the people in the disaster area. We sincerely pray for many persons passed away and are grateful to the cooperating persons in Kobe.

REFERENCES

- ERI (1995), "Hyogo-ken Nanbu earthquake, aftershock distribution", <http://www.eri-u-tokyo.ac.jp>.
- Fujita, K. and Kasama, T. (1982), *Geology of the Osaka-seihokubu district, with geological sheet map at 1:50000*, Geological Survey of Japan, Tukuba.
- Fujita, K. and Kasama, T. (1983), *Geology of the Kobe district, with geological sheet map at 1:50000*, Geological Survey of Japan, Tukuba.
- Hori, N. and Yamamoto, S. (1996), "Aftershock observation and source fault of the 1995 Kobe earthquake", *Bull. of Faculty of Engineering*, Kokushikan University, 29, pp.20-40.
- Katao, H, Maeda, N., Hiramatu, Y, Iio, Y. and Nakao, S. (1997), "Detailed mapping of focal mechanisms in/around the 1995 Hyogo-ken Nanbu earthquake rupture zone", *J. Phys. Earth*, 45,2, pp.105-119.
- Kikuchi, M. (1995), "The source mechanism by far field body wave", *The Earth (in Japanese)*, extra 13, 8 pp.47-53.
- Nakata, T. and Yomogida, K. (1995), "Surface faults characters of the 1995 Hyogo-ken Nanbu earthquake", *J.*

Nat. Disas. Sci., 16, pp.1-9.

Mizuno, K., Hattori, H, Sangawa, A. and Takahashi, H., (1990), *Geology of the Akashi district, with geological sheet map at 1:50000*, Geological Survey of Japan, Tokuba.

Research Group of Active Faults of Japan (1990), *Active faults in Japan*, The University of Tokyo Press, Tokyo.

Yamamoto, S. and Hori N. (1996), “ Aftershocks of the south Hyogo-prefecture earthquake”, *Special Issue on 1995 Hyogo-ken Nanbu earthquake*, Advanced research Center for Science and Engineering, Waseda University, B1, pp.37-43.

Yoshii,T. et al. (1973), “ Structure of southwest Japan margin off Shikoku”, *J. Geophys. Res.*, 78, pp.2517-2525.